Reactive Oxygen Intermediates Contribute to Necrotic and Apoptotic Neuronal Injury in an Infant Rat Model of Bacterial Meningitis Due to Group B Streptococci

Stephen L. Leib,* Young S. Kim,* Lucian L. Chow,* R. Ann Sheldon,‡ and Martin G. Täuber*‡

*Infectious Diseases Laboratory, San Francisco General Hospital, San Francisco, California 94110; and ‡Center for Neonatal Brain Disorders, Department of Medicine, Department of Neurology, and Department of Pediatrics, University of California San Francisco, San Francisco, California 94143

Abstract

Reactive oxygen intermediates (ROI) contribute to neuronal injury in cerebral ischemia and trauma. In this study we explored the role of ROI in bacterial meningitis. Meningitis caused by group B streptococci in infant rats led to two distinct forms of neuronal injury, areas of necrosis in the cortex and neuronal loss in the dentate gyrus of the hippocampus, the latter showing evidence for apoptosis. Staining of brain sections with diaminobenzidine after perfusion with manganese buffer and measurement of lipid peroxidation products in brain homogenates both provided evidence that meningitis led to the generation of ROI. Treatment with the radical scavenger α-phenyl-*tert*-butyl nitrone (PBN) (100 mg/kg q8h i.p.) beginning at the time of infection completely abolished ROI detection and the increase in lipidperoxidation. Cerebral cortical perfusion was reduced in animals with meningitis to $37.5\pm21.0\%$ of uninfected controls ($P < 0.05$), and PBN restored cortical perfusion to $72.0\pm8.1\%$ of controls ($P < 0.05$ vs meningitis). PBN also completely prevented neuronal injury in the cortex and hippocampus, when started at the time of infection ($P < 0.02$), and significantly reduced both forms of injury, when started 18 h after infection together with antibiotics ($P < 0.004$ for cortex and $P < 0.001$ for hippocampus). These data indicate that the generation of ROI is a major contributor to cerebral ischemia and necrotic and apoptotic neuronal injury in this model of neonatal meningitis. (*J. Clin. Invest.* 1996. 98: 2632–2639.) Key words: oxidative brain injury • lipidperoxidation • reactive oxygen intermediates • programmed cell death • cerebral cortical perfusion

Introduction

Reactive oxygen intermediates (ROI)[1] like superoxide anions and hydroxyl radicals can damage cells by oxidizing membrane phospholipids, proteins, nucleic acids, and nucleotides. ROI have been implicated in the pathogenesis of injury to neurons in a variety of central nervous system (CNS) insults, including cerebral inflammation (1), CNS trauma (2), ischemia-reperfusion injury (3), and glutamate mediated excitotoxicity (4). Several factors make the CNS particularly susceptible to oxidative damage. The brain receives $\sim 20\%$ of the cardiac blood output and has thus a high oxygen tension; brain cell membranes are rich in polyunsaturated fatty acids that can be oxidized by ROI; brain tissue has relatively low levels of endogenous antioxidant defense systems (e.g., superoxide dismutase, catalase, glutathione peroxidase) (5); and high concentration of iron in brain tissue promotes ROI generation (6, 7).

Bacterial meningitis continues to result in significant brain injury in many affected patients, despite the use of highly active antibiotics (8). In neonates, the patient population with the most severe form of bacterial meningitis, mortality rates can be as high as 30%, and up to 50% of surviving children are left with significant neurological sequelae (9). The mechanisms of CNS damage during meningitis have not been conclusively identified, but several lines of evidence indicate that ROI may contribute to brain injury. Inflammation has been strongly linked to the development of brain injury in experimental models of meningitis, and the major inflammatory cells in bacterial meningitis are neutrophilic granulocytes, which are potent generators of ROI (1). Inflammatory involvement of the cerebral vasculature has been suggested to be a major contributor to ischemic brain injury during meningitis (10), and cerebral vascular reactivity has been shown to be modulated by ROI in experimental meningitis (11, 12). Finally, neuronal injury in meningitis is in part caused by increased concentrations of excitatory amino acid (13, 14), and the neurotoxic effect of excitatory amino acids has been clearly linked to the generation of ROI (15–17). Despite these indirect lines of evidence linking the generation of ROI to the pathophysiology of meningitis, more direct evidence for a causative role of ROI in the development of neuronal injury has yet to be established.

Spin trapping agents react with ROI to form relatively stable adducts which in turn can be detected by spin resonance spectroscopy (15). α-phenyl-*tert*-butyl nitrone (PBN) has been used for the detection of ROI in various experimental systems (18). Only recently has PBN been discovered to have a beneficial effect on oxidative injury of the CNS. PBN administration protected rats from ischemic, traumatic, and excitotoxic brain injury and reduced endotoxin induced mortality (2, 7, 19–24). PBN showed no toxicity at the dosage used and the brain concentrations have been demonstrated to be significantly higher than those in blood (25). The high CNS penetration of PBN, a result of its lipophilicity, makes this compound an attractive tool to explore the role of ROI in various diseases that lead to brain injury. In the present study, we used an infant rat model of neonatal meningitis, in which extensive brain injury develops, to explore the hypothesis that meningitis leads to the generation of ROI, that PBN can reduce the generation of ROI,

---

---

1. *Abbreviations used in this paper:* CNS, central nervous system; CSF, cerebrospinal fluid; DAB, diaminobenzidine; GBS, group B *streptococcus*; PBN, α-phenyl-*tert*-butyl nitrone; ROI, reactive oxygen intermediates.

---

and that scavenging of ROI by PBN exerts a neuroprotective effect.

Methods

Infecting organism. A group B *streptococcus* type III (GBS; generously provided by Dr. Craig Rubens, University of Washington, Seattle, WA), one of the most common types causing neonatal meningitis, was used as described previously (14, 26). The organism was cultured overnight in Todd Hewitt broth, then diluted in fresh medium, grown to logarithmic phase, pelleted, and resuspended in normal saline to the desired density and used for infection.

Model of meningitis. Nursing Sprague-Dawley rat pups with their dam were purchased (Simonsen, Gilroy, CA) and infected on postnatal day 11 by direct intracisternal injection of 10 μl of a suspension of GBS, using a 32-gauge needle as described in (26). The inoculum size was 1×10^6 cfu/ml in the pretreatment group ($n = 20$) and between 1×10^5 to 1×10^6 cfu/ml in the posttreatment group ($n = 52$). 18 h after infection, pups were weighted and assessed clinically. To document meningitis, 10 μl of cerebrospinal fluid (CSF) was obtained by puncture of the cisterna magna, and cultured quantitatively. In a subset of animals, white blood cell (WBC) count was assessed in CSF samples by standard hematocytometer method. Animals were then treated with the antibiotic ceftriaxone (Hoffmann-La Roche, Nutley, NJ), 100 mg/kg subcutaneously once daily. Animals were killed with an overdose of pentobarbital at the predetermined timepoints or when they became terminally ill (cyanotic, difficulty breathing, protracted seizures). Animals dying unobserved were excluded from the evaluation.

Bacterial cultures. Serial dilutions of CSF in saline were cultured on blood agar plates incubated for 24 h at 37°C with 5% CO_2. In one experiment, infected animals were pretreated with PBN (100 mg/kg i.p. every 8 h, $n = 5$) or saline ($n = 5$) and killed immediately after the cisternal tap. 10 μl of blood was drawn from the left cardiac ventricle and cultured in parallel with the CSF samples. To assess a possible effect of PBN on bacterial growth, GBS was cultured overnight in Todd Hewitt broth, then equally diluted in fresh medium without ($n = 2$) or with PBN (Aldrich Chem. Co., Milwaukee, WI) at 10 mM ($n = 3$). This concentration corresponds to the maximally effective concentration protecting neurons from glutamate-induced toxicity in vitro (19), and exceeds the concentration of PBN in the CNS after a dose of 150 mg/kg i.p. in rats (25). After incubating all cultures for 210 min at 37°C with 5% CO_2, the density of the organisms was determined by quantitative subcultures.

Detection of ROI. For direct demonstration of the production of ROI in vivo, a cytochemical method previously described for the detection of superoxide in cerebral inflammation was adapted (1). Infant rats (seven uninfected controls; eight infected animals, and four infected animals pretreated with PBN, 100 mg/kg i.p. every 8 h) were perfused with 40 ml of citrate buffer containing 40 mM of manganese ($MnCl_2$) at the time of death. Brains were immediately frozen on dry ice, sectioned in a cryostat, and mounted on gelatinized slides. Sections where then incubated with a citrate buffer containing $MnCl_2$ (40 mM) and 1 mg/ml diaminobenzidine (DAB; Sigma Chemical Co., St. Louis, MO), counterstained with methyl green, air dried, and coverslipped. The brownish color reaction was used to assess ROI production, and was documented by photography.

Lipidperoxidation. The concentrations of malonaldehyde and 4-hydroxyalkenals, the endproducts of lipidperoxidation, provide a reliable index of the extent of oxidative damage to cell membranes (27, 28). Rat pups were randomly assigned to three experimental groups. Uninfected controls ($n = 8$), infected animals ($n = 8$), and animals infected and pretreated with PBN (100 mg/kg i.p. every 8 h; $n = 6$) were killed 20 h after infection. Brains were placed in ice-cold Tris-HCl (pH 7.4), the cortices were dissected, washed, snap frozen in liquid nitrogen, and stored at −70°C. 400 mg tissue was homogenized and diluted in Tris-HCl to 25% (wt/vol) on ice. After centrifugation at

3,000 g for 10 min at 4°C, 200 μl of supernatant was assessed for the concentration of the lipidperoxidation endproducts using a lipid peroxidation assay kit (Calbiochem, San Diego, CA) following the manufacturers instructions. The reaction of either lipidperoxidation product with the chromogenic reagent yielded a stable endproduct after incubation at 45°C for 40 min. The reaction was stopped on ice and the absorbance was measured at 586 nm. Using standard curves generated with samples of malonaldehyde and 4-hydroxyalkenal, the concentration of the chromophore in the solutions was calculated and expressed as micromolar per milligram of tissue.

Histopathology. After a lethal dose of pentobarbital, animals were perfused via the left cardiac ventricle with 60 ml of 4% paraformaldehyde in phosphate-buffered saline (pH 7.4). For histopathological examination brains were postfixed overnight in 5 ml of 4% paraformaldehyde in PBS (pH 7.4) at 4°C, then placed in 30% sucrose in PBS and cut at 50-μm intervals on a vibratome (29). Sections were mounted on gelatinized glass slides for staining. After dehydration, sections were Nissl stained in cresyl violet, and slides were rehydrated and coverslips were fixed with Permount. For quantitative evaluation, sections were examined for cortical neuronal injury, defined as areas of decreased density of neurons or frank cortical necrosis. 12 cortical sections spanning the middle half of the brain were scored in each animal for the presence or absence of neuronal injury, as described elsewhere (14), and the average injury score for each individual animal was used for statistical analysis. Similarly, injury to the dentate granule cell layer of the hippocampus was scored in each section containing the structure (14). The histopathologic evaluations were performed by an investigator blinded to the clinical, microbiological, and treatment data of animals.

Time-course experiments. To determine the optimal timepoint for pharmacological interventions, we assessed the earliest timepoint and the evolution of histopathologically discernible neuronal injury in the model. Animals ($n = 18$) were killed at predetermined timepoints (4, 12, 18, 20, 22, 24, and 36 h) and evaluated histopathologically, as described above.

Detection of apoptosis in situ. Infected animals ($n = 6$) were killed at 18, 24, and 36 h after infection together with age-matched controls ($n = 3$). Brains were processed as described for histopathological evaluation but postfixed for only 2 h. Three alternate sections of the midbrain region were cut at 50-μm intervals. One section was used for morphological evaluation by Nissl staining and two sections (sample and negative sham-stained control) were processed for the in situ detection of cells containing high amounts of fragmented DNA using a commercially available apoptosis detection kit (ApopTag®; Oncor, Gaithersburg, MD). Briefly, labeling of 3′-OH DNA ends visualized pyknotic nuclei with stainable concentration of DNA fragments as described (30). Digoxigenin-nucleotide residues added to the 3′-OH end of the DNA by terminal deoxynucleotidyl transferase were recognized by peroxidase conjugated antidigoxigenin antibodies. The localized peroxidase enzyme generated a signal from DAB as the chromogen. After counterstaining with methyl green, positive cells were counted by lightmicroscopy and expressed as percentage of total cell count within the structure of the dentate granule cell layer. As a positive control we used sections of normal female rat mammary gland 3–5 d after weaning of the pups. Negative controls included sham-stained sections (Terminal deoxynucleotidyl transferase substituted with distilled water) and tissue from uninfected animals.

Assessment of cerebral cortical perfusion. We examined cerebral cortical perfusion by intracardiac injection of the freely diffusible dye neutral red (Sigma Chemical Co.) using modifications of published procedures (31–34). Animals were infected with $\log_{10}$ 5.8±0.2 cfu/ml or injected with saline and treatment with PBN (100 mg/kg i.p. q 8 h) was started at the time of infection. Animals were anesthetized by intraperitoneal injection of sodium pentobarbital (100 mg/kg) at 20 h after infection, and 1 ml of a 3.6% solution of neutral red in saline (pH 7.0, twice filtered) was perfused through the contracting left cardiac ventricle over 45 s at a constant rate (1.36 ml/min). 75 s after the end of the infusion, rats were decapitated and brains harvested

and placed on dry ice. Cortical sections were cut on a cryostat at 50 μm and mounted on gelatinized glass slides. For computer-assisted quantitation of the dye density, sections were scanned on a flat bed scanner (Color One Scanner; Apple Computer, Cupertino, CA) and the digitized images were analyzed using the public domain NIH Image program (U.S. National Institutes of Health, Bethesda, MD). Mean cortical dye density in infected animals was expressed as percentage of density in uninfected control animals.

Effect of PBN on neuronal injury. The effect of PBN on neuronal injury scores in the infant rat model of neonatal meningitis was examined in two experiments. To attenuate ROI-mediated processes early in the course of meningitis and to maximize the effect of treatment, animals were randomized to pretreatment with PBN (100 mg/kg i.p. every 8 h ; $n = 10$) or saline ($n = 10$) in a first set of experiments. Animals were examined clinically, CSF cultures were obtained 18 h after infection, and brain injury scores were assessed between 22 and 24 h after infection. To evaluate the effect of delayed PBN administration on the outcome in fully developed meningitis, treatment was started together with antibiotics at 18 h after infection. PBN (100 mg/kg i.p., $n = 28$) or saline ($n = 24$) was administered at 18 h after infection (simultaneously with the first dose of ceftriaxone), 22, 26, 30 h and then continued with a dosing interval of 8 h until animals were killed 48 h after infection.

Statistics. Bacterial titers and lipidperoxidation endproducts are presented as mean ± SD and differences between groups were analyzed by Student's *t* tests. Proportions between different groups were compared by Fisher's exact test. Scores between groups were compared by the Mann-Whitney rank sum test.

Results

Characterization of the disease. By 18 h after infection, all infected animals had meningitis, as evidenced by positive bacterial titers in the CSF. Treatment of animals with PBN, beginning at the time of infection, led to CSF bacterial titers that were significantly higher than in untreated infected animals ($\log_{10}$ 10.1±0.7 cfu/ml vs $\log_{10}$ 8.0±0.4 cfu/ml; $P < 0.001$). Blood cultures performed in selected animals with meningitis showed a consistent 100-fold reduction in blood titers relative to the CSF titers, both in saline-treated control animals and in animals treated with PBN, and thus a higher level of bacteremia in PBN-treated animals than in controls ($P < 0.02$). The increased bacterial titers in the PBN-treated animals did not appear to result from a growth-promoting effect of PBN, since PBN at 10 mM had no significant effect on bacterial growth in vitro ($\log_{10}$ 8.9±1.2 vs 9.1±0.6 cfu/ml; $P = $ NS). CSF leukocyte counts showed no significant difference between infected animals treated with PBN and those treated with saline (6,420±7,255 vs 7,720±7,585 cells/mm^3; $P = $ NS). This suggests that the mechanism, by which PBN treatment leads to increased bacterial titers is related to scavenging of ROI produced by inflammatory cells, rather than to a negative effect on the recruitment of leukocytes into the CSF. Clinically, animals with meningitis were lethargic to obtunded 18 h after infection, with no obvious difference between animals treated with PBN and saline. In the posttreatment experiments, CSF bacterial titers at the time of institution of therapy were identical in the two experimental groups ($\log_{10}$ 8.7±0.7 vs 8.7±0.4 cfu/ml; $P = $ NS).

In histopathologic studies, the first granulocytes were seen in the subarachnoid space 4 h after intracisternal infection. CSF inflammation was fully developed by 18 h and always involved both the subarachnoid and ventricular space. Nissl staining with cresyl violet revealed two distinct forms of neu-

ronal injury, necrotic cortical injury and selective injury to the dentate gyrus of the hippocampus. In the cortex, the injury pattern consisted of areas of reduced neuronal density with neurons displaying morphologic features of necrosis, including cell swelling and loss of cytoarchitecture (Fig. 1 *A*). Foci of neuronal injury appeared throughout the cortex and tended to be wedge-shaped and thus suggestive of ischemic damage (Fig. 1 *B*). The earliest evidence of injury appeared in animals examined 18 h after infection, where one animal had incomplete, band-like areas of reduced neuronal density with intact neurons in the core of the lesions (26), while the two other animals studied at this time point had no evidence of neuronal drop out. All infected animals studied at subsequent time points in this experiment had evidence of injury, with the foci of necrosis becoming more extensive in animals studied after 22 h or later.

The pattern of injury in the hippocampus was distinctly different from that in the cortex. Beginning 18 h after infection, neurons in the granule cell layers of the dentate gyrus, predominantly in the lower blade, became markedly condensed, rounded and shrunken, showing morphological features characteristic for apoptosis (Fig. 1 *C*). Staining by in situ end-labeling of fragmented DNA, a hallmark of apoptosis, revealed positive cells bilaterally in the dentate granule cell layer of the hippocampus, with a predominance in the lower blade (Fig. 1 *D*). The stain was exclusively detectable in nuclei showing morphological signs of apoptotic death by Nissl stain (Fig. 1 *C*). Within the granule cell layer, the percentage of positive neurons were 8.6±3.3%. Other structures in the hippocampus, specifically the CA1 and CA3 region showed no positively stained cells and no evidence of neuronal damage by Nissl stain. Occasionally, single cells ($< 1\%$ of all cells) were positive in the cortex in areas of cortical injury. In addition, many inflammatory cells in the subarachnoid and ventricular space were positive. No positive signal was detected in uninfected animals and in infected animals showing no injury to the hippocampal dentate granule cell layer.

Production of ROI and oxidative brain injury. Evidence for the production of ROI in meningitis was obtained by the detection of superoxide in vivo by the manganese/DAB (DAB) method (1). Meningitis led to the generation of superoxide in all infected, untreated animals examined 18 h after infection ($n = 8$). Superoxide-derived DAB polymers colocalized with the inflammatory cells (predominantly granulocytes) in the subarachnoid and ventricular space and were also consistently seen along penetrating cortical vessels (Fig. 1 *E*). In one animal, foci of early cortical injury showed scattered individual cells positive for DAB polymers within the superficial brain parenchyma (Fig. 1 *F*). Their size and localization indicated that these cells were distinct from neurons (Fig. 1 *F*). In an additional animal, the dentate gyrus was markedly positive bilaterally. None of the infected animals treated with PBN ($n = 4$) showed DAB polymers ($P < 0.01$ vs infected, untreated animals) documenting that PBN effectively bound and neutralized ROI produced by the meningitic process. Also, all uninfected control animals ($n = 7$) were manganese/DAB staining negative.

Meningitis also led to a marked increase of the concentration of the lipid peroxidation endproducts malonaldehyde and 4-hydroxyalkenals 18 h after infection. In infected animals, the concentrations of these two products in homogenized brain tissue was 4.0±0.5 μM/mg tissue ($n = 8$), compared with 2.3±0.5
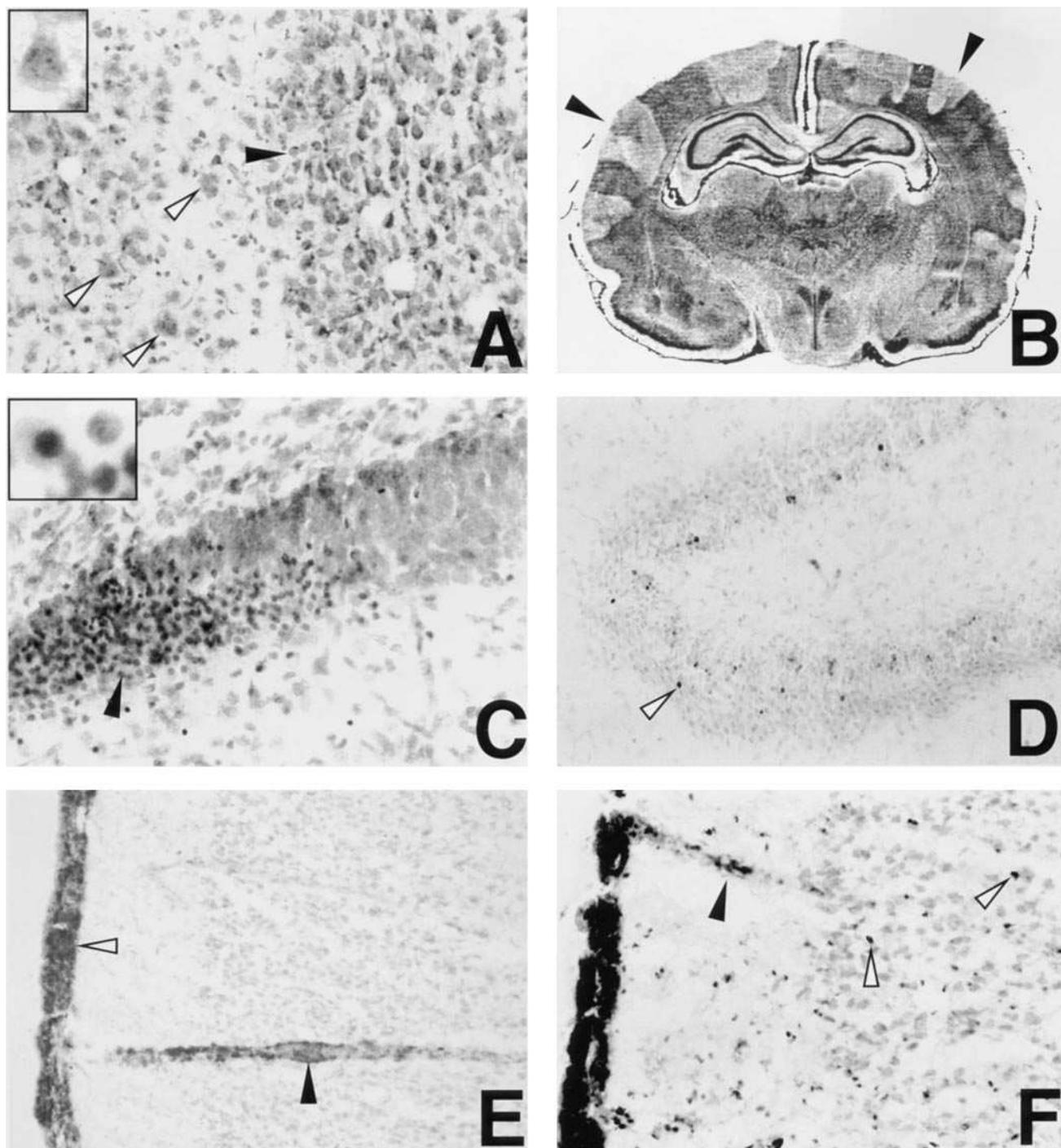
Figure 1. (*A–F*) Brain histology of saline treated infant rats with group B streptococcal meningitis. (*A*) Cortical injury in an animal 24 h after infection. Area of markedly reduced neuronal density containing neurons with morphologic features of necrosis, including cell swelling, loss of cellular demarcation, and fading of cytoarchitecture (*white arrows and inset*). Focus of neuronal loss is sharply demarcated from area with preserved neurons (*black arrow*). (Cresyl violet, ×400; *inset* ×1,200). (*B*) Whole brain section of an animal 36 h after infection showing extensive neuronal injury throughout the cortex in a wedge-shaped pattern suggestive of ischemic damage (*black arrows*). (Cresyl violet, ×5). (*C*) Neuronal injury to the lower blade of the dentate granule cell layer in the hippocampus of an animal 36 h after infection. Part of the blade consists of neurons with condensed, shrunken, and eccentric nuclei (*black arrow and inset*) showing morphological features compatible with apoptosis. Uninjured neurons of the structure are visible in the right upper quadrant. (Cresyl violet, ×400; inset ×2,000). (*D*) Staining by in situ end-labeling of fragmented DNA, a hallmark of apoptosis, revealed positive cells bilaterally in the dentate granule cell layer of the hippocampus (*white arrows*) in an animal 24 h after infection. A positive signal was exclusively detectable in nuclei showing morphological signs of apoptotic death by staining with cresyl violet. (ApopTag® peroxidase kit, counterstained with methyl green, ×200). (*E*) ROI production visualized by manganese/DAB method was seen in association with the subarachnoid space inflammation (*white arrow*) and along penetrating cortical vessels (*black arrow*). (DAB, counterstained with methyl green, ×200). (*F*) In an area of early cortical injury, individual cells showed positive staining for superoxide production by the manganese/DAB method (*white arrows*) in addition to the positive signals in the subarachnoid space and the cortical vasculature (*black arrow*). The DAB-positive cells appear to be smaller than and distinct from neurons. (DAB, counterstained with methyl green, ×400).

μM/mg tissue in uninfected animals ($n = 8$; $P < 0.001$). Pretreatment of infected animals with PBN ($n = 6$) completely prevented this increase in brain lipidperoxidation products (2.2 ± 0.2 μM/mg tissue; $P < 0.001$ vs infected, untreated animals; $P = $ NS vs uninfected controls).

Effect of PBN on cerebral cortical perfusion. In animals with meningitis ($n = 6$), cortical perfusion, as determined by assessing the mean optical dye density in cortical sections, was significantly reduced to $37.5\pm21.0\%$ of uninfected controls ($n = 4$; $P < 0.05$). Treatment with PBN ($n = 10$) significantly improved cortical perfusion ($72.0\pm8.1\%$ of uninfected controls; $P < 0.05$ vs infected, untreated animals, NS vs uninfected controls).

Effect of PBN treatment on neuronal injury. In a first set of experiments, we initiated therapy with PBN at the time of infection to maximize the potentially beneficial effects of PBN on neuronal injury. Five of 10 (50%) infected, saline-treated control animals showed histopathological evidence of neuronal injury in the cortex. All five animals also had damage in the hippocampus. Pretreatment with PBN (100 mg/kg q8h i.p.) completely abolished the development of brain injury ($P < 0.02$, Fig. 2, *A* and *B*). This protective effect was seen despite the significantly higher CSF bacterial titers in the animals treated with PBN (see above). PBN treatment in uninfected control animals had no clinical or histopathological effects.

The second set of experiments was performed to explore whether delayed administration of PBN still protected the brain from injury. Our time-course experiments (see above) indicated that the earliest histopathologic evidence of neuronal injury in this model appeared approximately 18 h after infection, and that there was noticeable progression of the extent of injury in the next few hours. The progression of injury was also evident from the comparison of control animals examined at 24 h (Fig. 2) with those examined at 48 h (Fig. 3). We therefore initiated treatment with antibiotics in combination with PBN or saline at 18 h, with the assumption that an effective treatment would prevent some, but not all injury. Injury scores (median and range) in the infected control animals were 1.6 (0–7) for cortical injury and 0.4 (0–3.7) for hippocampal injury. The extent of injury was significantly reduced by PBN treatment: 0.03 (0–4.5) for cortical injury ($P < 0.004$, Fig. 3 *A*), and 0 (0–1.3) for hippocampal injury ($P < 0.001$, Fig. 3 *B*). Thus, initiation of PBN treatment at a time point where

Figure 3. Effect of PBN (100 mg/kg PBN q4h - q8h i.p.) on neuronal injury in the cortex (*A*) and hippocampus (*B*), when started at 18 h after infection, at the time of institution of antibiotic therapy. PBN was highly protective for both forms of injury, the necrotic injury in the cortex, and the apoptotic injury in the dentate gyrus.

neuronal injury started to appear was still highly effective in preventing progression of injury.

Discussion

ROI have been implicated as mediators of brain injury in a wide variety of disease processes, including chemically induced cerebral inflammation (1), ischemia/reperfusion injury (6, 7, 22), brain edema (12, 35), neuronal apoptosis (36–39), and excitotoxic neuronal injury (4, 40–42). Pathophysiologic processes characteristic of bacterial meningitis, such as vascular endothelial cell activation and neutrophil adherence, subarachnoid space inflammation, blood-brain barrier disruption, brain edema, and excitotoxicity may also involve the generation of ROI (1, 35, 39, 43, 44). The present study provides strong evidence that ROI-mediated processes are critical in bacterial meningitis, and that inactivation of ROI by binding to the free radical scavenger PBN is a highly effective strategy to reduce neuronal damage in this disease.

Conceptionally, the course of bacterial meningitis can be divided into three phases. First, invading microorganisms generate an inflammatory response in the subarachnoid space; second, the cerebral vasculature reacts to the inflammation with cerebral hyperemia, followed later by cerebral ischemia; and third, cellular and molecular changes in the brain parenchyma lead to permanent brain injury. The generation of an inflammatory reaction, including the transcriptional regulation of cytokines and the expression of adhesion molecules on endothelial cells necessary to recruit granulocytes have been shown to involve ROI (43, 44). Nevertheless, CSF white blood cell counts were not significantly affected by the treatment with PBN, and histopathologic examination of the subarachnoid and ventricular inflammation also failed to show an obvious effect of pretreatment with PBN on the extent of inflammation in the present study. It appears therefore that PBN exerted its beneficial effects by mechanisms other than reducing the extent of CSF inflammation. With regard to the prospects of developing a drug such as PBN for the adjunctive therapy of bacterial meningitis, this may represent an advantage, since CSF inflammation is typically well developed, when patients with meningitis seek medical attention.

At the site of inflammation, activated polymorphonuclear leukocytes produce high concentrations of ROI (1). This was

Figure 2. Effect of PBN (100 mg/kg PBN q8h i.p.), beginning at the time of infection, on neuronal injury in the cortex (*A*) and hippocampus (*B*). In saline-treated control animals, GBS meningitis led to histopathological evidence of neuronal injury in the cortex and hippocampus of 50% of animals. Pretreatment with PBN (100 mg/kg q8h i.p.) completely abolished the development of brain injury.

confirmed in our studies using Mn/DAB staining, which showed markedly positive signals that colocalized with the inflammatory cells in the subarachnoid space and was abolished by PBN treatment. Treatment with PBN started at the time of infection abolished completely the detection of ROI by manganese/DAB staining and resulted in 100-fold higher CSF bacterial titers 18 h later. This suggests that ROI produced in the CSF space play a role as host defense mechanism against the group B streptococci. This is a new finding that contrasts with previous studies, where the absence of granulocytes, apparently the major source of ROI in the CSF, did not increase the growth rate or final titers of *pneumococci* (45, 46). This discrepancy may indicate that ROI produced in the subarachnoid space by cells other than neutrophils contribute to host defenses against bacterial pathogens, or that group B *streptococci* are more susceptible to the bactericidal effect of ROI than *pneumococci*. Importantly for the scope of the present study, the higher CSF bacterial titers were not associated with increased brain injury, indicating that bacteria per se, without the mediation of inflammation, cause little, if any damage.

Inflammation in the subarachnoid space surrounds blood vessels and can extend into the cortical parenchyma along the perivascular Virchow-Robins spaces. ROI production localized to the brain vasculature in the cortex was clearly demonstrated in the present study. During cerebral inflammatory states, endothelial cells and vascular smooth muscle cells have been identified as cellular sites of ROI production in the rat brain microvasculature (1). The colocalization of ROI production with cerebral blood vessels suggests that ROI may contribute to the changes of cerebral blood flow observed during bacterial meningitis (10, 47). In a study in rats using a cranial window preparation, exposure of pial arterioles to live and killed GBS produced a marked and progressive vasodilatation which was prevented by ROI scavengers (11). Similarly, ROI scavengers reduced the early hyperemia and brain edema in an adult rat model of pneumococcal meningitis (35). Whether prevention of this early hyperemia by scavengers of ROI is an important component of the neuroprotective effect of PBN was not addressed in the present study. ROI can also contribute to endothelial cell lesions that lead to the disruption of the blood–brain barrier and facilitate neutrophil adherence (35). PBN administration early in meningitis is likely to improve some of these potentially deleterious effects of inflammation and microcirculatory derangements.

As meningitis advances, cerebral blood flow starts to decline (48, 49), and clinical studies have found an association between severe cerebral blood flow reduction and adverse outcomes (50–52). Cerebral blood flow reduction during meningitis can be global, as a result of reduced cerebral perfusion pressure (49), or focal. Vasculitis of cerebral arteries and veins caused by the surrounding subarachnoid space inflammation may lead to temporary vasospasm or to permanent thrombosis, resulting in focal cerebral ischemia (10, 47, 53). The pronounced ROI production associated with the cerebral vasculature and the marked restitution of cerebral cortical perfusion by PBN in our model indicate that ROI play a critical role in the vascular events during meningitis that lead to cerebral hypoperfusion. Processes that may be attenuated by inactivation of ROI through scavenging with PBN include vasomotor responses, leukocyte–endothelial cell interactions, platelet activation, and intracranial pressure (11, 35, 44, 54). The improvement of cerebral perfusion resulting from scavenging of ROI

conceivably is an important reason for the neuroprotective effect of PBN in the present model, particularly when PBN was started at the time of infection and thus largely prevented the development of cerebral ischemia.

Cerebral ischemia leads to an increase in extracellular concentrations of excitatory amino acids, which results in excessive activation of neuronal receptors and excitotoxic cell death (40, 42). Previous studies documented that excitotoxicity plays a role in mediating neuronal injury in bacterial meningitis (13, 55). The production of excitotoxic neuronal injury is tightly linked to the generation of ROI, in that stimulation of neurons with excitatory amino acids leads to the production of ROI (15, 40), and that induction of oxidative injury in the hippocampus by exposure to ROI-generating substrates leads to the release of excitatory amino acids (42). Furthermore, activation of glial cells, an early event in bacterial meningitis (Leib, S.L., and M.G. Taüber, unpublished observations), involves the generation of ROI (56, 57). Exposure of glia to ROI has been shown in vitro to block clearance of excitatory amino acids by inhibiting specific uptake mechanisms (58). The link between oxidative and excitotoxic injury has the potential to lead to a vicious circle, which may propagate injury even after the initiating insult has been removed (42). Consequently, scavengers of ROI consistently attenuate excitotoxic injury in vitro and in vivo (4, 41). It is likely that a component of the beneficial effect of PBN in our model is related to the scavenging of ROI in ischemically injured brain parenchyma, particularly when PBN treatment was instituted in well established meningitis.

Our study has provided evidence for two distinct forms of neuronal injury. In the cortex, foci of neuronal injury showed many features suggestive of ischemic damage, such as wedge-shaped lesions, swollen neuronal cell bodies with loss of cytoarchitecture, and association with vascular involvement. In contrast, injury in the dentate granule cell layer of the hippocampus showed features characteristic for apoptosis. Several lines of evidence have recently supported a role for ROI in causing apoptosis in neurons (36, 37). In the immature rat, neurons of the hippocampal dentate granule cell layer were among the first to undergo apoptotic cell death in a recent study of hypoxic–ischemic injury, with the characteristic morphology and DNA fragmentation observed as early as 10 h after the hypoxic insult (59). Both forms of injury in our meningitis model, necrotic cortical injury and apoptotic hippocampal injury were markedly attenuated by treatment with PBN. This suggests that for both forms of neuronal injury ROI production is critical, even though the detailed mechanisms of ROI-mediated injury may well differ between the two forms.

Even though all infected animals had meningitis and evidence of oxidative injury, not all developed brain injury. This does, however, not exclude a critical role of ROI in causing brain injury in this model. First, the development of histologically apparent injury was time dependent, and in the after-treatment experiments almost all animals had some degree of injury. Second, there is almost invariably a range of severity of changes in animal models such as ours. For example, the concentrations of lipidperoxidation products in our study ranged from 3.3 to 4.9 μmol/mg tissue, the lower values being only slightly higher than the upper range of uninfected animals, despite the uniform presence of meningitis in the infected animals. Inspection of brain slices stained with DAB indicated that, while all animals had positive signals, their extent also was variable. Thus, the fact that not all animals had injury, par-

ticularly at the earlier time point studied, seems to reflect the variability inherent in animal models, rather than argue against a causative role of ROI in brain injury in this model of meningitis.

In summary, this study documents a critical role of ROI production in the pathogenesis of neuronal injury in a model of neonatal GBS meningitis. We have localized the generation of ROI primarily to cells constituting the subarachnoid and ventricular inflammation and to the cerebral vasculature, and have documented the occurrence of lipidperoxidation. Furthermore, inhibition of the biological effect of ROI with the free radical scavenger PBN significantly improved cerebral cortical perfusion and reduced the extent of both necrotic and apoptotic neuronal injury. This is the first report to demonstrate a significant beneficial effect of a radical scavenger on the neuropathologic outcome in bacterial meningitis.

Acknowledgments

References

1. Kontos, C.D., E.P. Wei, J.I. Williams, H.A. Kontos, and J.T. Povlishock. 1992. Cytochemical detection of superoxide in cerebral inflammation and ischemia. *Am. J. Physiol.* 263:H1234–H1242.

2. Sen, S., H. Goldman, M. Morehead, S. Murphy, and J.W. Phillis. 1994. Alpha-phenyl-tert-butyl-nitrone inhibits free radical release in brain concussion. *Free Radical Biol. & Med.* 16:685–691.

3. Defraigne, J.O., O. Detry, J. Pincemail, C. Franssen, M. Meurisse, M. Lamy, and R. Limet. 1994. Direct evidence of free radical production after ischemia and reperfusion and protective effect of desferrioxamine: ESR and vitamin E studies. *Eur. J. Vasc. Surg.* 8:537–543.

4. Schulz, J.B., D.R. Henshaw, D. Siwek, B.G. Jenkins, R.J. Ferrante, P.B. Cipolloni, N.W. Kowall, B.R. Rosen, and M.F. Beal. 1995. Involvement of free radicals in excitotoxicity in vivo. *J. Neurochem.* 64:2239–2247.

5. Cohen, G. 1988. Oxygen radicals and Parkinson's disease. *In* Oxygen Radical and Tissue Injury. B. Hallimell, editor. FASEB/USA, Bethesda, MD. 130–135.

6. Nelson, C.W., E.P. Wei, J.T. Povlishock, H.A. Kontos, and M.A. Moskowitz. 1992. Oxygen radicals in cerebral ischemia. *Am. J. Physiol.* 263:H1356–H1362.

7. Carney, J.M., and R.A. Floyd. 1991. Protection against oxidative damage to CNS by α-phenyl-*tert*-butyl nitrone (PBN) and other spin-trapping agents: a novel series of nonlipid free radical scavengers. *J. Mol. Neurosci.* 3:47–57.

8. Durand, M.I., S.B. Calderwood, D.J. Weber, S.I. Miller, F.S. Southwick, V.S. Caviness, and M.N. Swartz. 1993. Acute bacterial meningitis in adults: a review of 493 episodes. *N. Engl. J. Med.* 328:21–28.

9. Edwards, M.S., M.A. Rench, A.A.M. Haffar, M.A. Murphy, M.M. Desmond, and C.J. Baker. 1985. Long-term sequelae of group B streptococcal meningitis in infants. *J. Pediatr.* 106:717–722.

10. Pfister, H.W., G.D. Borasio, U. Dirnagl, M. Bauer, and K.M. Einhäupl. 1992. Cerebrovascular complications of bacterial meningitis in adults. *Neurology.* 42:1497–1504.

11. McKnight, A., W. Keyes, M. Hudak, and M. Jones. 1992. Oxygen free radicals and the cerebral arteriolar response to group B streptococci. *Pediatr. Research.* 31:640–644.

12. Pfister, H.W., U. Koedel, S. Lorenzl, and A. Tomasz. 1992. Antioxidants attenuate microvascular changes in the early phase of experimental pneumococcal meningitis in rats. *Stroke.* 32:1798–1804.

13. Guerra-Romero, L., J.H. Tureen, M.A. Founrier, V. Makrides, and M.G. Täuber. 1993. Amino acids in cerebrospinal and brain interstitial fluid during experimental pneumococcal meningitis. *Pediatr. Res.* 33:510–513.

14. Leib, S.L., Y.S. Kim, D.M. Ferriero, and M.G. Täuber. 1996. Neuroprotective effect of excitatory amino acid antagonist kynurenic acid in experimental bacterial meningitis. *J. Infect. Dis.* 173:166–171.

15. Lafon-Cazal, M., S. Pietri, M. Culcasi, and J. Bockaert. 1993. NMDA-dependent superoxide production and neurotoxicity. *Nature (Lond.).* 364:535–537.

16. Reynolds, I.J., and T.G. Hastings. 1995. Glutamate induces the production of reactive oxygen species in cultured forebrain neurons following NMDA receptor activation. *J. Neurosci.* 15:3318–3327.

17. Dugan, L.L., S.L. Sensi, L.M.T. Canzoniero, S.D. Handran, S.M. Rothman, T.-S. Lin, M.P. Goldberg, and D.W. Choi. 1995. Mitochondrial production of reactive oxygen species in cortical neurons following exposure to *N*-methyl-D-aspartate. *J. Neurosci.* 15:6377–6388.

18. Kalyanaraman, B. 1982. Detection of toxic free radicals in biology and medicine. *Rev. Biochem. Toxicol.* 4:73–139.

19. Yue, T.-L., J.-L. Gu, P.G. Lysko, H.-Y. Cheng, F.C. Barone, and G. Feuerstein. 1992. Neuroprotective effects of phenyl-t-butyl-nitrone in gerbil global brain ischemia and in cultured rat cerebellar neurons. *Brain Res.* 574:193–197.

20. Novelli, G.P. 1992. Oxygen radicals in experimental shock: effects of spin-trapping nitrones in ameliorating shock pathophysiology. *Crit. Care Med.* 20:499–507.

21. French, J.F., T.E. Craig, T.R. Downs, D.F. Ohlweiler, A.A. Carr, and R.C. Dage. 1994. Protective effects of a cyclic nitrone antioxidant in animal models of endotoxic shock and chronic bacteremia. *Circ. Shock.* 43:130–136.

22. Cao, X., and J.W. Phillis. 1994. α-phenyl-tert-butyl-nitrone reduces cortical infarct and edema in rats subject to focal ischemia. *Brain Res.* 644:267–272.

23. Zhao, Q., K. Phalmark, M.-L. Smith, and B.K. Siesjoe. 1994. Delayed treatment with the spin trap alpha-phenyl-N-tert-butyl nitrone (PBN) reduces infarct size following transient middle cerebral artery occlusion in rats. *Acta Physiol. Scand.* 152:349–350.

24. Folbergrova, J., Q. Zaho, K.-I. Katsura, and B.K. Siesjoe. 1995. N-tert-butyl-α-phenylnitrone improves recovery of brain energy state in rats following transient focal ischemia. *Proc. Natl. Acad. Sci. USA.* 92:5057–5061.

25. Cheng, H.-Y., T. Liu, G. Feuerstein, and F.C. Barone. 1993. Distribution of spin trapping compounds in rat blood and brain: in vivo microdialysis determination. *Free Radical Biol. & Med.* 14:243–250.

26. Kim, Y.S., R.A. Sheldon, B.R. Elliot, Q. Liu, D.M. Ferriero, and M.G. Täuber. 1995. Brain damage in neonatal meningitis caused by group B streptococci in rats. *J. Neuropathol. Exp. Neurol.* 54:531–539.

27. Esterbauer, H., and K.H. Cheeseman. 1990. Determination of aldehydic lipid peroxidation products: malonaldehyde and 4-hydroxynonenal. *Methods Enzymol.* 186:407–421.

28. Melchiorri, D., R.J. Reiter, E. Sewerynek, L.D. Chen, and G. Nistico. 1995. Melatonin reduces kainate-induced lipid peroxidation in homogenates of different brain regions. *Fed. Am. Soc. Exp. Biol.* 9:1205–1210.

29. Ferriero, D.M., S.M. Sagar, L.J. Arcavi, T.K. McIntosh, and R.P. Simon. 1988. Selective sparing of NADPH diaphorase neurons in neonatal hypoxia-ischemia. *Ann. Neurol.* 24:670–677.

30. Gavrieli, Y., Y. Sherman, and S.A. Ben-Sasson. 1992. Identification of programmed cell death in situ via specific labeling of nuclear DNA fragmentation. *J. Cell Biol.* 119:493–501.

31. Selman, W.R., A.J. Ricci, R.C. Crumrine, J.C. LaManna, R.A. Ratcheson, and W.D. Lust. 1990. The evolution of focal ischemic damage: a metabolic analysis. *Metab. Brain Dis.* 5:33–44.

32. Selman, W.R., C. VanDerVeer, T.S. Whittingham, J.C. LaManna, W.D. Lust, and R.A. Ratcheson. 1987. Visually defined zones of focal ischemia in the rat brain. *Neurosurgery (Baltimore).* 21:825–830.

33. LaManna, J.C., and K.A. McCracken. 1984. The use of neutral red as an intracellular pH Indicator in rat brain cortex in vivo. *Anal. Biochem.* 142:117–125.

34. Griffith, J.K., B.R. Cordisco, C.-W. Lin, and J.C. LaManna. 1992. Distribution of intracellular pH in the rat brain cortex after global ischemia as measured by color film histophotometry of neutral red. *Brain Res.* 573:1–7.

35. Koedel, U., A. Bernatowicz, R. Paul, K. Frei, A. Fontana, and H.-W. Pfister. 1995. Experimental pneumococcal meningitis: cerebrovascular alterations, brain edema, and meningeal inflammation are linked to the production of nitric oxide. *Ann. Neurol.* 37:313–323.

36. Rothstein, J.D., L.A. Bristol, B. Hosler, R.H. Brown Jr., and R.W. Kuncl. 1994. Chronic inhibition of superoxide dismutase produces apoptotic death of spinal neurons. *Proc. Natl. Acad. Sci. USA.* 91:4155–4159.

37. Troy, C.M., and M.L. Shelanski. 1994. Down-regulation of copper/zinc superoxide dismutase causes apoptotic death in PC12 neuronal cells. *Proc. Natl. Acad. Sci. USA.* 91:6384–6387.

38. Rabizadeh, S., E.B. Gralla, D.R. Borchelt, R. Gwinn, J.S. Valentine, S. Sisodia, P. Wong, M. Lee, H. Hahn, and D.E. Bredesen. 1995. Mutations associated with amyotropic lateral sclerosis convert superoxide dismutase from an antiapoptotic gene to a proapoptotic gene: studies in yeast and neuronal cells. *Proc. Natl. Acad. Sci. USA.* 92:3024–3028.

39. Bonfoco, E., D. Krainic, M. Ankarcrona, P. Nicotera, and S.T. Lipton. 1995. Apoptosis and necrosis: two distinct events induced, respectively, by mild and intense insults with *N*-methyl-D-aspartate or nitric oxide/superoxide in cortical cell cultures. *Proc. Natl. Acad. Sci. USA.* 92:7162–7166.

40. Yang, C.-S., N.-N. Lin, P.-J. Tsai, L. Liu, and J.-S. Kuo. 1996. *In vivo* evidence of hydroxyl radical formation induced by elevation of extracellular

glutamate after cerebral ischemia in the cortex of anesthetized rats. *Free Radical Biol. & Med.* 20:245–250.

41. Patel, P., B.J. Day, J.D. Crapo, I. Fridovich, and J.O. McNamara. 1996. Requirement for superoxide in excitotoxic cell death. *Neuron.* 16:345–355.

42. Pellegrini-Giampietro, D.E., G. Cherici, M. Alesiani, V. Carla, and F. Moroni. 1990. Excitatory amino acid release and free radical formation may co-operate in the genesis of ischemia-induced neuronal damage. *J. Neurosci.* 10:1035–1041.

43. Schwartz, M.D., J.E. Repine, and E. Abraham. 1995. Xanthine oxidase-derived oxygen radicals increase lung cytokine expression in mice subjected to hemorrhagic shock. *Am. J. Respir. Cell Mol. Biol.* 12:434–440.

44. Lo, S.K., K. Janakidevi, L. Lai, and A.B. Malik. 1993. Hydrogen peroxide-induced increase in endothelial cell adhesiveness is dependent on ICAM-1 activation. *Am. J. Physiol.* 264(4 Pt 1):L406–L412.

45. Täuber, M.G., U. Borschberg, and M.A. Sande. 1988. Influence of granulocytes on brain edema, intracranial pressure, and cerebrospinal fluid concentrations of lactate and protein in experimental meningitis. *J. Infect. Dis.* 157:456–464.

46. Ernst, J.D., J.M. Decazes, and M.A. Sande. 1983. Experimental pneumococcal meningitis: role of leukocytes in pathogenesis. *Infect. Immun.* 41:275–279.

47. Förderreuther, S., K. Tatsch, K.M. Einhäupl, and H.W. Pfister. 1992. Abnormalities of cerebral blood flow in the acute phase of bacterial meningitis in adults. *J. Neurol.* 239:431–436.

48. Täuber, M.G., M. Burroughs, U.M. Niemöller, H. Kuster, U. Borschberg, and E. Tuomanen. 1991. Differences of pathophysiology in experimental meningitis caused by three strains of *Streptococcus pneumoniae. J. Infect. Dis.* 163:806–811.

49. Tureen, J.H., M.G. Täuber, and M.A. Sande. 1992. Effect of hydration status on cerebral blood flow and cerebrospinal fluid lactic acidosis in rabbits with experimental meningitis. *J. Clin. Invest.* 89:947–953.

50. Ashwal, S., W. Stringer, L. Tomasi, S. Schneider, J. Thompson, and R. Perkin. 1990. Cerebral blood flow and carbon dioxide reactivity in children with bacterial meningitis. *J. Pediatr.* 117:523–530.

51. Goitein, K.J., and I. Tamir. 1983. Cerebral perfusion pressure in central nervous system infections of infancy and childhood. *J. Pediatr.* 103:40–43.

52. Odio, C.M., I. Faingezicht, M. Paris, M. Nassar, A. Baltodano, J. Rodgers, X. Saez-Llorens, K.D. Olsen, and G.H.J. McCracken. 1991. The beneficial effects of early dexamethasone administration in infants and children with bacterial meningitis. *N. Engl. J. Med.* 324:1525–1531.

53. Thomas, V.H., and I.J. Hopkins. 1972. Arteriographic demonstration of vascular lesions in the study of neurologic deficit in advanced *Haemophilus influenzae* meningitis. *Dev. Med. Child. Neurol.* 14:783–787.

54. Ikeda, H., Y. Koga, T. Oda, K. Kuwano, H. Nakayama, T. Ueno, H. Toshima, L.H. Michael, and M.L. Entman. 1994. Free oxygen radicals contribute to platelet aggregation and cyclic flow variations in stenosed and endothelium-injured canine coronary arteries. *J. Am. Coll. Cardiol.* 24:1749–1756.

55. Perry, V., R.S.K. Young, W.J. Aquilla, and M.J. During. 1993. Effect of experimental *Escherichia coli* meningitis on concentrations of excitatory and inhibitory amino acids in the rabbit brain: in vivo microdialysis study. *Pediatr. Res.* 34:187–191.

56. Chao, C.C., S. Hu, and P.K. Peterson. 1995. Modulation of human microglial cell superoxide production by cytokines. *J. Leukocyte Biol.* 58:65–70.

57. Masana, Y., T. Yoshimine, T. Fujita, M. Maruno, E. Kumura, and T. Hayakawa. 1995. Reaction of microglial cells and macrophages after cortical incision in rats: effect of a synthesized free radical scavenger, (+/−)-N,N′-propylenedinioctinamide (VAS). *Neurosci. Res.* 23:217–221.

58. Volterra, A., D. Trotti, C. Tromba, S. Floridi, and G. Racagni. 1994. Glutamate uptake inhibition by oxygen free radicals in rat cortical astrocytes. *J. Neurosci.* 14:2924–2932.

59. Beilharz, E.J., C.E. Williams, M. Dragunow, E.S. Sirimanne, and P.D. Gluckmann. 1995. Mechanisms of delayed cell death following hypoxic-ischemic injury in the immature rat: evidence for apoptosis during selective neuronal loss. *Mol. Brain Res.* 29:1–14.